

Introduction to Radio Astronomy

P. Hily-Blant

2020-21

Contents

1	Summary	1
2	Introduction	2
2.1	The radio sky	2
2.2	Radio astronomy: measurement of noise power	2
2.3	Basic characteristics of radio telescopes	3
2.4	Telescope gallery	3
3	Coherent receivers	4
3.1	Overview	4
3.2	Coherent receiver components	5
3.3	Dual-band receivers	8
4	Frequency conversion and sidebands	8
4.1	The mixer (2): frequency conversion	9
4.2	Sidebands	9
5	Beam pattern	10
5.1	Optics	10
5.2	The antenna beam pattern	10
5.3	What do radio telescopes measure?	11
5.4	Observing modes	12
6	Temperature scales	12
6.1	The antenna temperature	12
6.2	The main-beam temperature	13
6.3	Noise and the radiometer formula	13
7	Bolometers	13

1 Summary

- Radio astronomy covers the long wavelength part of the electromagnetic spectrum, with λ larger than ~ 0.1 mm, and up to ionospheric plasma frequency at 40 MHz.
- The power from radio astronomical is \approx fW; to have a chance to detect these signals, they must be amplified to mW (120 dB) and time integration from few s to hours may be required.
- The variance of the measured signal is given by the radiometer formula;

- There are two broad categories of detectors

- Coherent, which measure the amplitude and phase of the wave from the astrophysical source, and incoherent ones, similar in principle to calorimeters, which measure the total energy within a broad-band $\Delta\nu \sim 0.3\nu$ around a given frequency ν ;
- Today, both types are superconducting receivers, and are operated at low temperature (~ 4 K) using cryostats;
- Coherent receivers:
 - * they can reach extremely high spectral resolution power $R=\nu/\delta\nu \sim 10^6$ or even larger
 - * their noise temperature (similar to dark current in CCD) is limited by the quantum noise $h\nu/k$; today, $T_{\text{rec}} \approx$ few $h\nu/k$.
 - * they are made of several components: a horn, waveguides, a mixer, a local oscillator, and amplifiers
 - * the mixer is the superconducting part; it has two functions: perform the frequency down-conversion from the radio frequency (RF, 100-1000 GHz) to the intermediate frequency (IF, typically 4-8 GHz)
 - * their phase-preserving capacity is essential in interferometry and allows to recover the interference term and therefore to obtain image reconstruction with high fidelity.

- Antenna beam pattern

- The beam pattern is the radiation diagram of the optics+receiver; the beam pattern is, in general, a two-dimensional function;
- The finite size of the optics (the pupil) leads to oscillation in the beam pattern; these are called sidelobes;
- By proper design of the receiver horn, the sidelobes can be attenuated and the beam pattern be well approximated by a Gaussian.

- A telescope delivers the convolution of the source brightness distribution by the power pattern (or PSF)
- Temperatures in radioastronomy
 - The antenna temperature is the convolution of the sky brightness and the antenna beam pattern
 - When the source is of a size comparable to the main beam of the telescope, the main-beam temperature scale is the most appropriate; if the source was a black-body then the Rayleigh-Jeans corrected T_{mb} would be the temperature of the black-body;
- Radio astronomy has a lot of jargon inherited from the radio engineering community; one has to get used to it.

References: Lazareff 2000 (Proceedings of the IRAM Interferometry School), Carter et al 2012 A&A, Phillips and Woody 1982 ARAA, Wengler et al 1992 IEEE, Essential Radio Astronomy (Condon and Ransom)

2 Introduction

2.1 The radio sky

As can be seen in Fig.1, the radio sky is dominated, at cm wavelengths, by continuous spectra as opposed to line spectra. A unique exception is the 21cm line of atomic hydrogen at 1420 MHz. At much lower intensity, molecular lines are also routinely measured with modern radio telescopes at cm to submm wavelengths.

Continuous radio emission is primarily due to synchrotron emission from relativistic electrons gyrating in galactic magnetic fields radiating, and by thermal bremsstrahlung in HII regions. At shorter wavelengths, in the far infrared, thermal emission is dominated by heated dust grains. In between, 13.7 Gyr old photons from the last scattering surface are the main source of emission.

2.2 Radio astronomy: measurement of noise power

What do radio telescopes measure? Both optical and radio telescopes observe the electromagnetic field emitted by extraterrestrial sources. However, there is a sharp difference in what they actually measure.

Radio astronomy, that is, detection of long wavelength radiation from extraterrestrial sources, started with the discovery by Karl Jansky (1932) of radio waves from the galactic center. The detection of a *noise-like* signal with a period of 23h56, the sidereal period, indicated that the



Figure 1: On May 5th 1933, the New York Times reports the discovery of radio waves from extraterrestrial sources. Learn more [here](#).

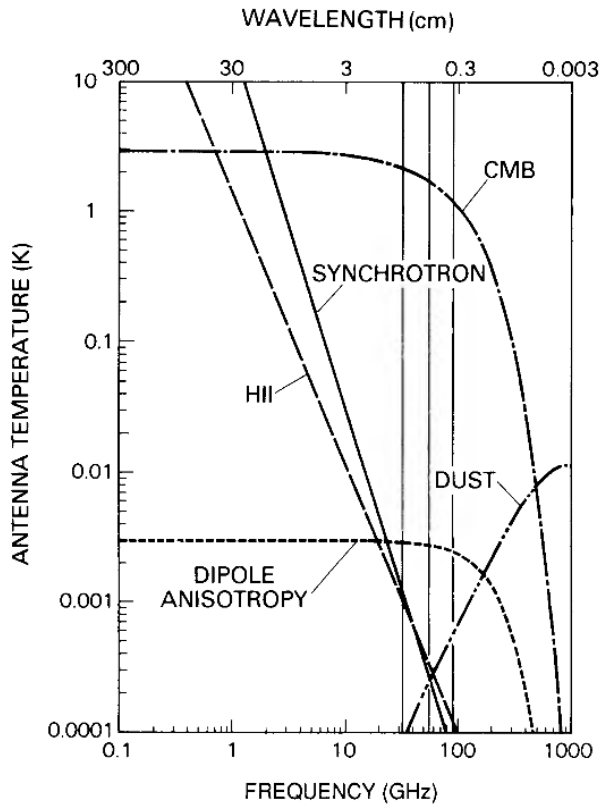


Figure 2: The important sources of emission at radio wavelength, in antenna temperature $T_A = c^2 I_\nu / (2k\nu^2)$ (see Section 6). From Smoot et al 1990.

signal was not terrestrial. At the time, Jansky was *listening*¹ to the output of the receiver and noted that the regular output was a "hiss", a 'noise' familiar to radio engineers, typical of what is emitted by a (warm) resistance. Extraterrestrial waves are indeed also called 'radio noise', in reference to continuous signals, common in radio engineering, as opposed to sharp spectral lines.

At visible wavelength, the intensity of a source, which is measured directly—integrated over a range of wavelength or in wavelength-dependent fashion when a spectrometer is used—dominates over the dark surroundings. On the other hand, radio telescopes do not measure the intensity of the incident wave but instead, they are sensitive to the electric field incoming onto the dish. The noise-like nature of radio signals is a consequence of the temperature dependence of the black-body, namely that $B_\nu(T_1) > B_\nu(T_2), \forall \nu$ iff $T_1 > T_2$. If the source has an effective temperature (the temperature one has to plug into the black-body radiation to simulate the same specific intensity) much larger than the surroundings of the telescope and the atmosphere, then the signal is dominated by the source. On the other hand, if the source has a low T_{eff} —and this is often the case in radio astronomy because λT_{eff} is constant—then the surroundings, which have temperatures typically above 50K and up to ambient (300 K), will dominate: but black-body radiation over

a small bandwidth has no spectral feature and is random in nature hence taking the shape of a noise.

2.3 Basic characteristics of radio telescopes

When a radio telescope is pointed towards a discrete source, the output voltage (or current) is increased with respect to the value without a source. The flux density (F_ν) of the unresolved source is proportional to the voltage increase. The conversion from voltages to flux density is called *calibration*. As will be seen later, if the source flux density is S , then the power increment measured by the antenna is

$$p = 1/2 A_e S$$

with A_e the **effective area**, which is less than the geometrical area. A_e is measured by the staff of the telescope. The flux density is the flow of energy from the source through a unit area in the wavefront at the observing point, per unit spectral range and per unit time. Hence, **S is measured in $\text{W Hz}^{-1} \text{m}^{-2}$** . In radio astronomy, signals are usually extremely weak, and a the **Jansky unit** is usually more suitable:

$$1 \text{ Jy} = 10^{-26} \text{ W Hz}^{-1} \text{m}^{-2}$$

An antenna is a **linear device**, meaning that the energy it delivers has a frequency equal to that of the incoming wave. An antenna is **intrinsically polarized**: they are sensitive to one polarization only, say linear. Hence, it can measure only half of the intensity. To recover the total intensity, a pair of antennas sensitive to perpendicular polarization (assuming they are linearly polarized) must be used. At mm wavelength, the **polarization selectivity is due to the horn**. Hence, it is customary to have two horns looking at the same position on the sky simultaneously; the incoming light is then splitted into two mutually perpendicular linearly polarized beams. This is achieved by using a beam-splitter that is made of a wired-grid, the reflected and transmitted beams are linearly polarized and perpendicular.

2.4 Telescope gallery

A selection of three radio telescopes is shown in Figs. 3-4. The first is the historical telescope used by A. Penzias and R. Wilson to measure the CMB radiation temperature (see [here](#) and [here](#)). This telescope is called a horn-reflector antenna because there is here no focussing optics such as in short wavelength (mm, submm) radio telescopes. It has an aperture area of 391 square feet (36 m^2). The CMB was measured at 4080 Mc/s, or 7.3 cm. The horn is typically a few times the wavelength. Here, it is much bigger because there is no optics. The gain of the horn reflector is $\approx 47.6 \text{ dB}$ ($\approx 6 \times 10^4$) at 4080 MHz. Such a very high gain illustrates a basic characteristic of radio astronomy as discussed previously: scientific signals are extremely weak and need to be amplified considerably to have a chance to detect them. Furthermore, this signal is

¹Because the output of the electrical device was coded as a sound.

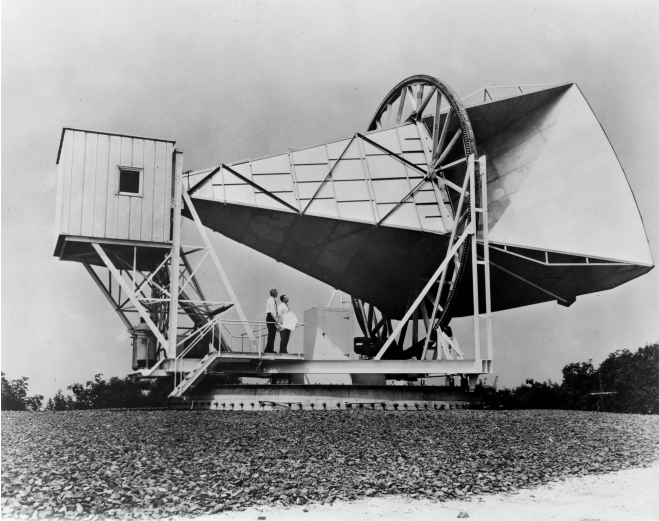


Figure 3: The horn-reflector telescope used by A. Penzias and R. Wilson to measure the CMB temperature.



Figure 4: The fully steerable Green Bank 100m telescope (Gregorian, off-axis; active optics).



Figure 5: The fully steerable IRAM-30m telescope (Cassegrain design).

lost in a forest of thermal emission which dominates at long wavelength (compared to visible wavelengths), and only by integrating over long timescales can the weak signal be isolated from the noise.

Figs. 4 and 5 show modern single-dish radiotelescopes, the 100-m **Green Bank Telescope**, and the **30m IRAM telescope**. Both are fully steerable using an alt-azimuthal mount. The optical design are quite distinct however: the GBT is a Gregorian with an off-axis secondary while the IRAM-30m is a Cassegrain. The advantage of the off-axis is to reduce aperture blockage by the secondary support. However, distortions of the diffraction pattern (the beam) must be corrected for. The GBT possesses an active control of its primary mirror which allows to correct for the aforementioned aberrations and also for gravitational distortion. The latter is compensated in the IRAM-30m by using a so-called homologous structure which ensures a parabolic shape upon deformation. The IRAM-30m possesses an elaborated thermal control of the structure and secondary support, ensuring high pointing accuracy and excellent focus, hence high sensitivity.

3 Coherent receivers

3.1 Overview

We distinguish two types of detectors, **coherent**, which measure the **amplitude** and **phase** of the incoming electromagnetic **wave**, and **incoherent** which register only the **energy** carried by the incoming wave, usually over a broad band. Incoherent receivers are also called *bolometers*, although calorimeter would often be more appropriate. All receivers in the mm and submm domains use superconducting devices for their higher sensitivity that is, their capability to detect faint signals.

In this Section, we will focus on **coherent receivers**. Coherent receivers are motivated by the aim of detecting **spectral lines** with high spectral resolution. These receivers are also called *superheterodyne receivers* (or simply, heterodyne), acknowledging the fact that all these devices are based on the frequency-mixing method.

If we focus ourselves on the detection devices rather than the optical design, a radiotelescope may be summarized as shown in Fig. 6. The signal from the sky (Radio Frequency, RF, at frequency ν_{sky}) is collected by the optics and is converted into a field propagating into **waveguides** by the **horn**, down-converted into the **mixer** whose output is a voltage at the intermediate frequency, with an **amplitude proportional to the power of the incoming wave** and a **phase that is preserved**. The voltage is amplified at low temperature (usually with a High Electron Mobility Transistor, **HEMT**) and further amplified at room temperature. The signal is finally sent into **spectrometers** which nowadays are essentially numerical.

The salient characteristics of heterodyne receivers are:

- low-noise amplification
- phase-preserving
- high spectral resolution (virtually unlimited), which reaches $R = \nu_{\text{sky}} / \delta\nu \sim 10^7$ below 1 THz;
- modest instantaneous bandwidth: $\Delta\nu \sim 0.1\nu_{\text{sky}}$
- covers the entire mm and submm up to $\nu_{\text{sky}} \approx 2$ THz
- sensitivity is limited by quantum noise limit: $T_{\text{rec}} > h\nu/k = 5\text{K}$ at 100 GHz.

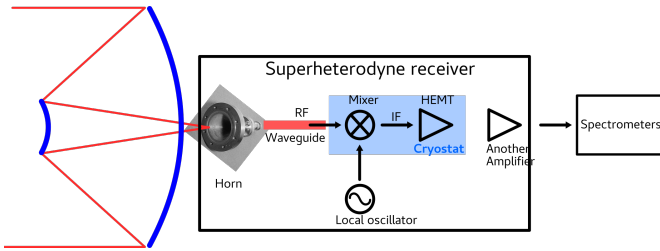


Figure 6: Overview of the various components of a superheterodyne radio telescope.

3.2 Coherent receiver components

The coherent receiver we will describe in what follows use Superconductor-Insulator-Superconductor (SIS) mixers. The main components are summarized in Fig. 6 which is an over-simplification of real receivers, while a real receiver is shown in Fig. 7:

- the **horn**: it receives the RF from the reflecting optics and illuminates the SIS mixer (actually the *junction*, in solid state physics terminology);
- the **waveguide**: they transport one mode of the electric field (e.g. TE₁₀) from the horn to the mixer;
- the **mixer**: it has two functions; (1) frequency down-conversion, from the so-called **radio frequency** (ν_{RF} , this is the frequency of the signal from the sky, say 100 GHz at $\lambda=3\text{mm}$) down to the **intermediate frequency** (ν_{IF} , usually a few GHz, typically 4 to 8 GHz); and (2) power measurement; as of today, mixers for mm-submm spectral line observations at frequency below 1THz use superconducting SIS mixers—an insulator sandwiched between two superconducting layers—and best performances are obtained at $\approx 4\text{K}$.
- the **low-noise amplifier** (HEMT): brings the IF signal to a level above the room temperature thermal noise; amplification may be done in several steps, the first being done at cryogenic temperatures. At IRAM, this is performed below 15K.

Let us now look at each part into little more details.

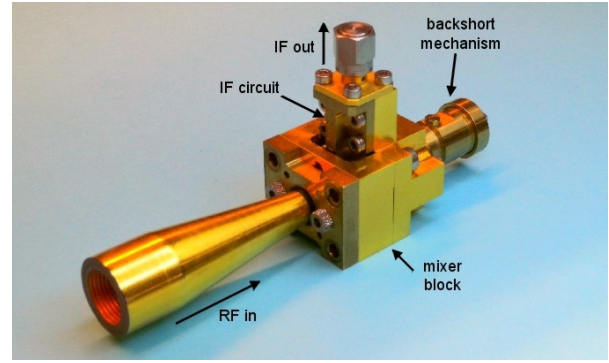


Figure 7: A complete mm SIS receiver developed at IRAM. The size is $\approx 5 \times 10\text{cm}$.

3.2.1 The horn

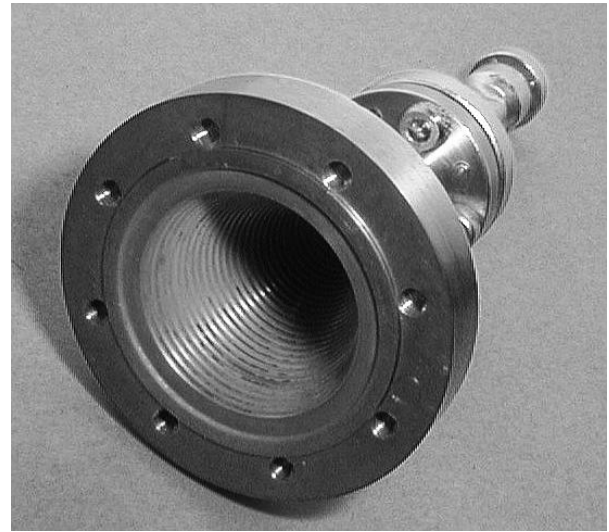


Figure 8: An example of a cylindrical, corrugated, horn.

The RF signal focussed by the optics is sent to the **feedhorn**. The purpose of the feedhorn is twofold:

- transform the incoming RF from free-space propagation in waveguide propagation
- apodization leading to attenuated sidelobes in the beam pattern (see Figs. 17 and 18).

In the mm and submm domains (but not only, see the horns developed for the COBE mission), the feedhorn is a cylindrical piece of metal, of entrance diameter $\sim 10 \lambda_{\text{sky}}$.

Very simply, diffraction at the sharp edges of the horn produce oscillations, called **sidelobes** in the diffraction pattern, which should be made as small as possible in order to maximise the directivity of the telescope. Strong sidelobes would collect signal from different incoming angles, including the ground or the receiver cabin itself, thus contaminating the scientific signal with a strong, time-dependent, thermal emission much stronger than the desired signal (or, in the case of the COBE measurements, its fluctuations). The reduction of unwanted signals from off the beam was a key to the success of the

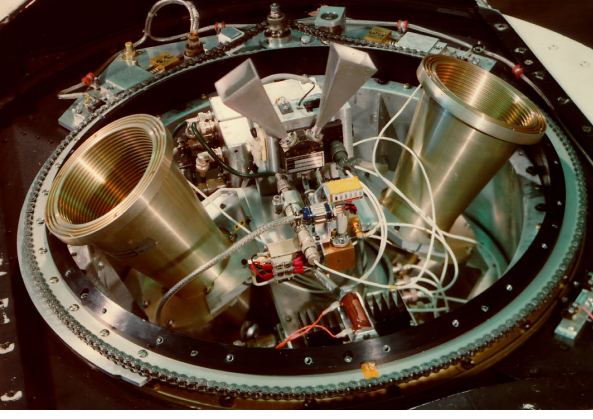


Figure 9: The Differential Microwave Radiometer (DMR) used in COBE to measure CMB anisotropy. Note the corrugated horns.

COBE experiment that led to the measurement of the CMB fluctuations spectrum (Nobel Prize 2006 to Smoot and Mather).

The problem is therefore the following: how to obtain the cleanest power pattern that is also frequency-independent (we wish to be able to cover a non-zero spectral range)?

One possibility is to use *aperture-matched horns*, which is similar to a trumpet or a trombone, where the edges are smoothly curved so as to cancel the electric field, and its derivative, at the edges. However, much better performances and more compact design achieve efficient sidelobes reduction and free-space-to-waveguide propagation conversion: these are *corrugated cylindrical horns* (see Figs. 8 and 9). In the case of the COBE/FIRAS horns, the depth of the corrugations is $\lambda/2$ at the entrance of the horn, and $\lambda/4$ in the inner part. These corrugations ensure that the electric field (ideally a plane wave) incident on the circularly symmetric primary is converted into the TE₁₀ mode of the rectangular waveguide.

3.2.2 The mixer (1): power measurement

We now describe the SIS mixer. The great advance and key feature of SIS mixers is that they can perform two, equally important and fundamental, operations:

- measure the power of the incident RF signal with quantum limited noise
- perform the so-called frequency down-conversion

In this Section, we first describe how the mixer can measure the power of the incoming wave. The frequency down-conversion will be addressed in the next Section.

1. Mixers as power detectors: basic physics The fundamental process involved in SIS junctions is the photon-assisted tunneling of quasi-particles in *superconducting* devices. This is quite similar to *semiconducting* photodetectors used in the visible or in

the infrared, where the bandgap is, however, of the order of 1 eV, much larger than the energy involved in the mm/submm domain (meV).

One important characteristic of a superconductor is its energy gap, 2Δ , to which is associated a gap voltage $V_{\text{gap}}=2\Delta/e$. In the mm/submm domain, the energy of the incoming radiation is $h\nu$ so that we wish to have $2\Delta \sim h\nu$, hence

$$V_{\text{gap}} = h\nu/e \quad (1)$$

which is ~ 0.4 meV at 100 GHz. The gap depends on the material used as a superconductor: 2.5mV for lead alloys, 3-5 mV for niobium and niobium alloys.

Two currents may manifest themselves in superconductors, which are associated to the motion of two types of charge carriers: quasiparticles and Cooper pairs.

A quasiparticle is, actually, a real particle, with charge $-e$. It is also called normal electron or single electron. The main difference, however, between a quasiparticle and an electron in a metal is the energy of the quasiparticles: their energy density of states has a gap of 2Δ .

Cooper pairs are single electrons with a binding energy 2Δ . These Cooper pairs are responsible for the zero-resistivity current in superconductors. The motion of Cooper pairs gives rise to the Josephson current. SIS are, indeed, also called Josephson junctions.

The signal of interest for astronomical observations is the one carried by the quasiparticles.

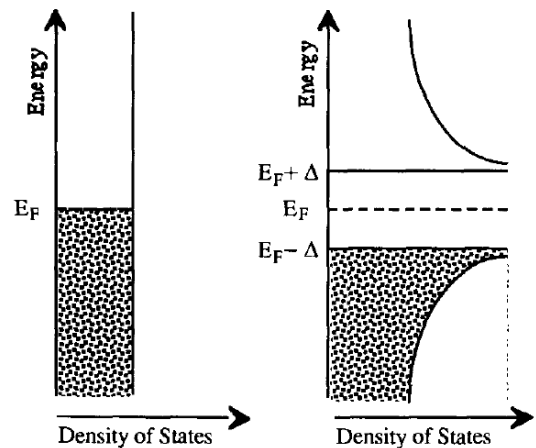


Figure 10: **Left:** The density of states of electrons in a conductor at 0K. **Right:** density of states of quasiparticles in a superconductor at 0K. In both panels, states below E_F (the Fermi energy) are occupied while those above are empty. (From Wengler 1992).

Superconductors and semiconductors have in common an energy gap in the energy density of states of

the electrons. For instance, the conduction band in semiconductors, above the energy gap, is similar to the empty continuum of states shown in Fig. 10. However, there are important differences between supra and semi:

- (a) The energy gap is of order 1eV in the latter, and ≈ 500 times smaller in the former
- (b) The shape of the density of states above the gap are different: the density increases as the energy increases in the semi, while it is maximum right above the gap in the supra and decreases as the energy of the quasiparticles increases;
- (c) In the supra, there are two types of currents, while in a semiconductor there is one, carried by holes and electrons.

SIS receivers were developed independently at Bell Labs for 115 GHz mixing (Dolan et al. 1979) and for 36 GHz (Richards et al. 1979) at Berkeley. SIS junctions have superseded the semiconducting hot electron bolometers (HEB) by offering instantaneous intermediate frequency (see later) bandwidth much larger than 1 MHz (the 1 MHz IF bandpass limit of HEB is set by the relaxation rate of the hot electrons). SIS junctions have proved to be the most effective receivers in the submillimeter band of 100-800 GHz and have been used in nearly all receivers in telescopes which work in this range. For this reason, we will only describe the general principles of heterodyne receivers using SIS junctions. We note also that Schottky diode receivers allow IF bandpass similar to SIS junctions but are characterized by poorer noise performances and have also been supplanted by SIS junctions in the mm/submm domain.

2. SIS junctions

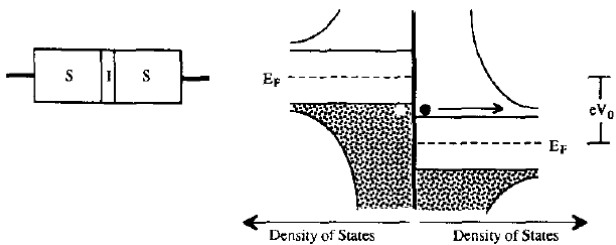


Figure 11: An SIS junction is a thin insulator between two superconducting layers. The Fermi energy of the two superconductors are separated by eV_0 where V_0 is the bias dc voltage. A quasiparticle has tunneled through the insulator, generating a current through the SIS.

SIS junctions are made of two superconductors separated by a thin (typically few nm) insulator (see

Fig. 11). For a current to flow across the junction, charge carriers must *tunnel* through the insulator. The insulator I must be thin enough such that the wavefunctions of the electrons in either S overlap sufficiently in I. Note that, because energy is conserved, the path of an electron in this type of diagram is a horizontal line. IRAM receivers use Niobium alloys for the superconductor, and Aluminium oxide for the insulator, with a typical cross-section $1\mu\text{m}^2$.

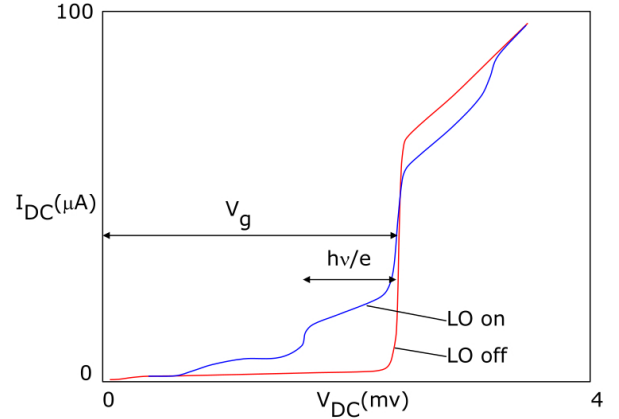


Figure 12: The I-V curve of a SIS without (LO off) and with (LO on) input signal.

3. SIS response and the dc voltage bias

In Fig. 11, electrons (in this qualitative discussion, it is sufficient to treat quasiparticles as electrons) can tunnel from left to right provided that they find the "conduction" band, at $E_F + \Delta$. If the energy difference between the left and right supra was less than shown in the plot, electrons would not be able to flow into the "valence" band on the right because it is already full, or because they would find themselves in the gap where there is no energy state. The dc voltage V_0 that is applied imposes a difference of eV_0 between the Fermi levels on either side.

The "LO off" curve in Fig. 12 shows the I-V curve of an SIS junction when there is no local oscillator input, i.e. the response of a pure SIS. When the dc voltage is increased, there is a sharp rise of the current at ≈ 2.5 mV which corresponds to the energy gap $2\Delta/e$. When V_0 is lower than V_{gap} , electrons from the valence band on the left encounter the gap: no current. When V_0 is just above V_{gap} , the current jumps. When V_0 is increased further, the increase is linear (this is the behaviour above the Curie temperature): more valence states from the left create more conduction states.

4. Photon-assisted tunneling

If we know apply a RF signal to the SIS junction, the I-V curve shows steps (blue curve in Fig. 12 This may be understood from Fig. 13. Absorption of a

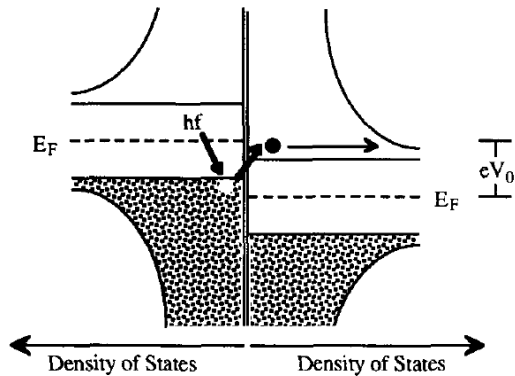


Figure 13: Photon-assisted tunneling. The energy of the incoming wave promotes a quasiparticle from one superconductor to the conduction band of the other.

RF photon by a valence electron on the left makes it capable of finding an empty state in the "conduction" band. Clearly, if one wishes to detect one photon of energy $h\nu_{\text{sky}}$, the voltage bias should be $V_{\text{gap}} - h\nu_{\text{sky}}/e$. If the number of photons was n , then the bias voltage satisfies:

$$V_{\text{gap}} - nh\nu_{\text{sky}}/e < V_0 < V_{\text{gap}} - (n-1)h\nu_{\text{sky}}/e \quad (2)$$

The increase of the current in Fig. 11 shows that it is stepwise, which is due to different values of the number of absorbed photons n .

The responsivity (ratio of the current generated over the absorbed power, similar to quantum efficiency of CCD) of SIS junctions is extremely good and is \approx one electron per photon.

5. Suppression of the Josephson current The current associated to the Cooper pairs is called Josephson current and produces additional noise. This unwanted Josephson current is suppressed by applying an external dc magnetic field, with so-called Josephson coils (see Fig. 14).

3.2.3 Waveguides

There are input and output waveguides. The purpose of the former is to bring the incoming radiation to the SIS junction which is placed perpendicular to its axis.

The typical cross-section of the waveguide is a fraction of the incoming wavelength, λ_{sky} . It may be rectangular, with typical dimensions 0.5×0.25 in units of λ_{sky} , the free-space wavelength. At 230 GHz, this is $\approx 600 \times 300 \mu\text{m}$. Rectangular waveguides can be used up to ~ 800 GHz. One important feature of rectangular waveguides is the good control of impedance matching between the telescope and the receiver, resulting in excellent beam patterns.

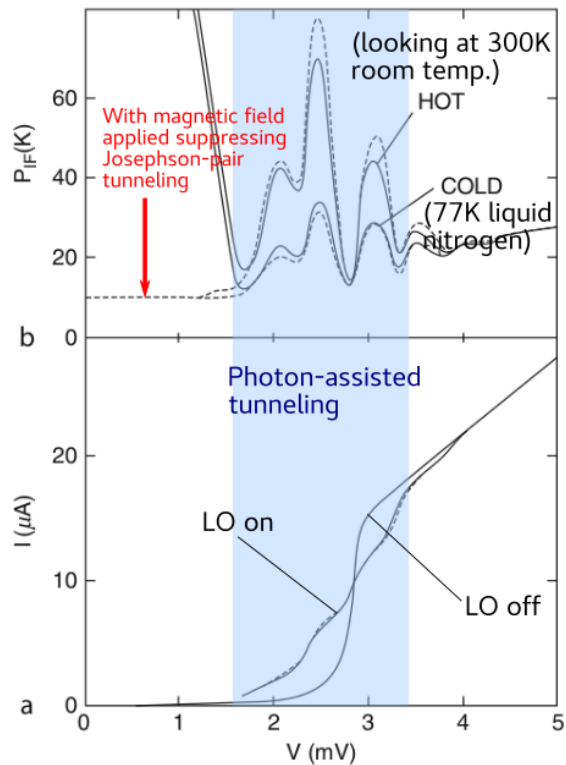


Figure 14: Photon-assisted tunneling and suppression of the Josephson current by applying an external magnetic field.

3.3 Dual-band receivers

Dual-channel receivers, such as those installed at the IRAM-30m telescope, allow to observe simultaneously with two receivers. This is accomplished with a Martin-Puplett Interferometer (MPI). The key point is that coherent receivers are *monomode* devices, hence they transmit a single polarization, which could be linear or circular. Since any polarization state can be decomposed linearly in two perpendicular polarizations, recovering the total intensity can be achieved by means of two receivers transmitting perpendicular polarizations. Another application could be to observe a given source simultaneously at two frequencies, e.g. the rotational transitions $J=1-0$ and $2-1$ of carbon monoxide, CO. Allowing such a situation is the aim of the MPI. Let us consider linear polarizations.

4 Frequency conversion and sidebands

We now switch to the second aspect of SIS mixers: the RF-to-IF frequency conversion. First, let us see briefly why we need this, and the basic idea of it. As will be seen, what makes the frequency conversion possible is the strongly non-linear I-V curve due to the sharp onset of quasiparticle current through the gap when the dc bias voltage is set close to the energy gap of the superconducting metals.

4.1 The mixer (2): frequency conversion

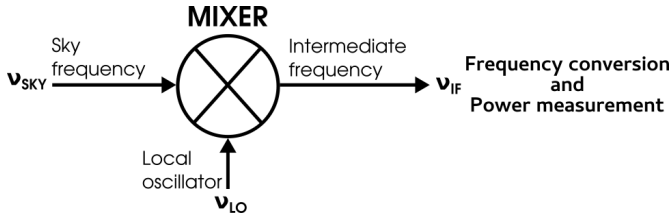


Figure 15: The RF-to-IF down conversion principle using non-linear mixing of the RF with LO signals.

Why do we need to convert the RF signal to a lower frequency? This is because electronic devices such as amplifiers or samplers do not have good performances at mm/submm frequencies (typically 100GHz or more). Furthermore, linear detectors would make averages of the incoming electric field over a response time τ which is most likely much larger than $1/\nu_{\text{sky}}$, thus leading to zero average (a 100 GHz sky frequency would require a response time much shorter than 10^{-12} s). Therefore, quadratic detectors are needed.

4.1.1 Frequency mixing

As said already, the mixer also performs the frequency down-conversion as summarized schematically in Fig. 15: the **radio frequency** (RF) and **local oscillator** (LO) signals are **added** first and then **multiplied**. The latter is made possible because of the non-linear I-V curve of a SIS junction close to threshold. Consider radiation incident on the SIS junction which generates a voltage V_{sky} ; the RF voltage across the mixer is

$$V_{\text{RF}}(t) = V_{\text{LO}} \cos(2\pi\nu_{\text{LO}}t) + V_{\text{sky}} \cos(2\pi\nu_{\text{sky}}t) \quad (3)$$

where $V_{\text{LO}} \gg V_{\text{sky}}$. The RF power absorbed in the mixer is proportional V_{RF}^2 . This gives rise to:

- two dc terms: $1/2(V_{\text{sky}}^2 + V_{\text{LO}}^2)$
- 2nd harmonics: $\cos(2\pi\nu_{\text{sky}}t + \phi)$ and $\cos(2\pi\nu_{\text{LO}}t + \phi')$;
- and to two terms: $\cos[2\pi(\nu_{\text{sky}} - \nu_{\text{LO}})t + \dots]$ and $\cos[2\pi(\nu_{\text{sky}} + \nu_{\text{LO}})t + \dots]$

After averaging over a time that is long compared to $1/\nu_{\text{sky}}$ and $1/\nu_{\text{LO}}$, and short compared to $1/(\nu_{\text{sky}} - \nu_{\text{LO}})$, the high-frequency terms vanish:

$$P_{\text{RF}}(t) = P_{\text{sky}} + P_{\text{LO}} + 2\sqrt{P_{\text{sky}}P_{\text{LO}}} \cos(2\pi\nu_{\text{IF}}t) \quad (4)$$

Receiving devices based on the frequency down-conversion are called *heterodyne receivers*, because the basic principle is that the RF is mixed with another signal, the LO. The latter is usually generated locally, next to the receiver.

Note that, in writing $P_{\text{RF}} \propto V_{\text{RF}}^2$, we have assumed that the junction is quadratic, i.e. we have neglected higher-order terms in the Taylor expansion of the non-linear I-V curve of the junction in terms of the voltage excursion from the dc bias $V_0 = V_{\text{gap}}$. However, these high-order terms can be made small by an appropriate choice of the bias voltage.

4.1.2 The intermediate frequency

The *intermediate frequency*, ν_{IF} , is defined by:

$$\nu_{\text{IF}} = |\nu_{\text{LO}} - \nu_{\text{sky}}| \quad (5)$$

Applying a bandpass filter would remove the dc components, leaving the IF term only.

What is important to realize is that the sky signal amplitude is multiplied by that of the LO, and that the intermediate frequency is set by the LO frequency. Therefore, by choosing ν_{LO} close to ν_{sky} , the IF can be made small. In practice, $\nu_{\text{IF}} \approx \text{few GHz}$. Why? The previous derivation was based on a monochromatic frequency ν_{sky} . However, heterodyne receivers based on SIS junctions will be sensitive to a RF bandpass which translates into a IF bandpass. There are many instances in which it is desirable to cover a broad bandpass $\Delta\nu$: spectral surveys of star forming regions, galaxies and other extragalactic sources having broad lines. Obviously, ν_{IF} must be of the order of the desired bandwidth. As of 2019, typical values for the IF bandpass is 4-8 GHz.

4.2 Sidebands

A consequence of the frequency down-conversion through non-linear mixing of the RF and LO signals is that to one intermediate frequency corresponds two sky frequencies:

$$\nu_{\text{sky}} = \nu_{\text{LO}} \pm \nu_{\text{IF}} \quad (6)$$

The upper sky frequency defines the *upper side band* (USB), while the lower frequency corresponds to the *lower side band* (LSB). There are three types of receivers:

- SSB: only one band (either LSB or USB, observatory dependent); the unwanted band is attenuated by means of a special type of interferometric filter called a Martin-Puplet interferometer.
- DSB: both bands superimposed
- 2SB: LSB and USB simultaneously *and* separated
- Sky frequency: $\nu_{\text{S}} = \nu_{\text{LO}} - \epsilon$ and $\nu_{\text{S}} = \nu_{\text{LO}} + \epsilon$ have the same IF frequency
- EMIR at IRAM are 2SB: use the phase sign difference between LSB and USB; instantaneous bandwidth of 32GHz (almost a bolometer !)

- Figure of merit for SSB and 2SB: band rejection (usually in dB) or image gain (dimensionless)

In SSB receivers, the band of the expected signal is called the *signal side band* while the other band is called the *image side band*. There is no convention and the signal side band may be the LSB or the USB, depending on the receiver used. In SSB receivers, the image side band is attenuated with a rejection coefficient, expressed in dB, which is of order 10dB or more. Recall that $\text{dB} = 10 \log_{10}(P_1/P_0)$, so a 10dB rejection means that the image side band is attenuated by a factor 10; 20dB corresponds to a factor 100. In SIS junction receivers, the rejection is usually achieved with a mechanical device called a *backshort*. An intuitive description of this can be found in Lazareff's Lecture.

Despite the potential degeneracy in line identification with DSB receivers, these devices have interesting features: first, they allow to observe twice as much a band-pass. In regions where the density of lines is not high, this can be interesting. Second, the atmospheric noise is divided by $\approx \sqrt{2}$. However, the advent of 2SB receivers (see, e.g. [Carter et al 2012](#)) has improved significantly the radio telescope capabilities.

5 Beam pattern

5.1 Optics

Radio telescopes are ruled by the same principles from physical optics and therefore of geometrical optics, as the more familiar optical wavelength telescopes. The main configurations are thus two-mirrors reflecting telescopes, with Cassegrain or Gregorian setup, hence having a parabolic primary. These configurations were described in more details in Chapter XX. However, Ritchey-Chrétien telescopes have not been designed at radio wavelengths, most likely because the need for large field of view is not such a concern. At cm wavelength, however, spherical primaries are also used, such as the Arecibo or FAST telescopes.

The Green Bank Telescope (GBT) is an example of an offset paraboloid telescope: a 100x110m section of a parent 208m diameter symmetric paraboloid ($f/D=0.29$), with a clear aperture thanks to an off-axis Gregorian secondary. The secondary is an ≈ 8 m diameter portion of an ellipsoid (100μ rms). This telescope is also equipped with an active control system (see Chapter Telescopes).

5.2 The antenna beam pattern

The propagation of the light, from a source to a pupil, is described by the Huyghens-Fresnel theory of diffraction. When the source is at a large distance d from the pupil this reduces to the Fraunhofer theory of diffraction. The

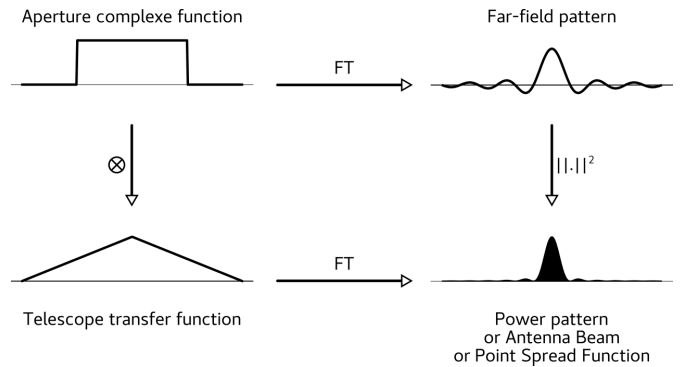


Figure 16: The relation between the power pattern and the aperture function, and the parallel view from visible wavelength telescope terminology. The telescope transfer function (or optical transfer function) is the autocorrelation product of the aperture (pupil) function.

far-field approximation is:

$$d \gg \pi D^2 / \lambda = 2827 \text{km} (D/30 \text{m})^2 (\lambda/1 \text{mm})^{-1} \quad (7)$$

where D is the diameter of the pupil and λ the wavelength. This is therefore readily the case, unless perhaps for some solar system objects observed with a 10km interferometer operating at short mm/submm wavelengths.

Let us consider that we use the antenna as an emitter instead of a detecting device. The invariance of the Maxwell equations under time reversal ensures that the derived properties will be equally valid.

Fraunhofer's theory states that the far-field electric field is the Fourier Transform of the electric field in the pupil:

$$E_{\text{ff}}(l, m) \propto \mathcal{F}[E_{\text{ant}}(x, y)]$$

At one dimension, a constant amplitude field applied over a length D would lead to a far-field electric field given by a sinc function.

Clearly, sharp edges of the pupil will inevitably generate oscillations in the radiation diagram. What is important to realize is that not all the power is then radiated in a focused beam but that there are also *sidelobes* or *minor lobes*: some power is radiated towards offset directions, and even behind the telescope (see Fig.17). In reception mode now, this means that the antenna would collect signal coming from not only the source, but also from other directions in the sky, from the ground or from the telescope itself. At optical wavelength, this is not as much a problem as in radio astronomy. At long wavelength, thermal emission emitted at low temperature is strong. Actually, the atmosphere is roughly a 70K blackbody, the ground is ≈ 300 K, while the source signal is usually a few K, or much less.

Vocabulary:

- Complex aperture function: the electric field in the pupil; also called aperture field function at optical wavelength;

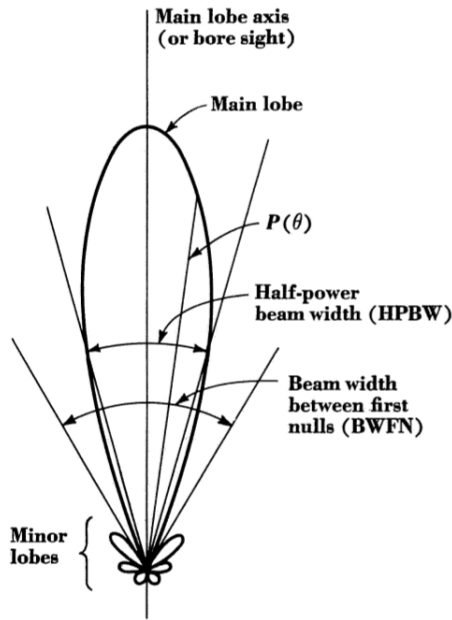


Figure 17: The general beam pattern of a radio telescope. The main lobe concentrates most of the energy. Minor lobes, or sidelobes, also receive some power from offset directions (other extraterrestrial sources, the atmosphere), including from the ground or the telescope itself. In practice, beams are made very nearly Gaussian by the use of corrugated horns.

- Far-field pattern: Fourier transform of the complex aperture function
- Power pattern: modulus of the far-field pattern

Definitions:

- Normalized power pattern noted $P(\theta, \phi)$, with $P(0,0)=1$. We will note $P(\omega) \equiv P(\theta, \phi)$.
- Beam solid angle:
 - $\Omega_A = \int_{4\pi} P(\Omega) d\Omega$
 - $\Omega_{mb} \leq 4\pi$, unless $P=1$
- Main-beam solid angle:
 - $\Omega_{mb} = \int_{\Omega_{mb}} P(\Omega) d\Omega \leq 4\pi$
 - This definition of Ω_{mb} is a usual one, but is not unique.
- Effective area:
 - $A(\theta, \phi) = A_e P(\theta, \phi) \leq A_e$
 - $A_e = \eta_a A_{geom}$, $0 \leq \eta_a \leq 1$ is the aperture efficiency;
- Fundamental relation (étendue, or throughput):
 - $A_e \Omega_A = \lambda^2$

The latter can be derived by the following thought experiment: the antenna is placed within an enclosure which is maintained at a temperature T , and we wait for thermodynamical equilibrium to be established within the enclosure. Therefore, the antenna receives as much power as it radiates. Per unit frequency, this means that:

$$1/2 \int_{4\pi} A(\omega) B_\nu(T) d\omega = kT \quad [\text{W}/\text{m}^2/\text{Hz}]$$

where the factor 1/2 comes from the fact the antenna will be sensitive to only one polarization of a transverse wave. The right-hand side follows from the Nyquist (1928) theorem which states that any resistance (also true for a complex one) at temperature T emits a monochromatic power kT . This is the case at long wavelengths, in the Rayleigh-Jeans domain, while this would have to multiplied by $[\exp(h\nu/kT)-1]^{-1}$ in the general case. If we consider again long wavelengths, we obtain the desired result, namely that the throughput is $A_e \Omega_A = \lambda^2$ which must be a general one, since our equation only involves properties of the antenna itself. At shorter wavelength, the same result is obtained since the radiated power would then also contain the $[\exp(h\nu/kT)-1]^{-1}$ correction.

It is interesting to realize what this relation means:

- An antenna having a diameter D will have a beam solid angle $\Omega_A \approx 2/\pi (\lambda/D)^2$; thus, an antenna with $D \gg \lambda$ is highly directive;
- Conversely, to have a nearly isotropic antenna, its diameter should be close to the wavelength;
- Actually, that $\Omega_A \approx (\lambda/D)^2$ is reminiscent of the PSF of a uniform circular aperture of diameter D has a FWHM $1.028 \lambda/D$. However, the throughput relation is an exact equality, so the nature of the two relations are fundamentally different, as our derivation may suggest.

5.2.1 Example of a Gaussian beam pattern

Let us consider a power pattern given by $P(\theta, \phi) = \exp(-\theta^2/2\sigma^2)$ that is, an azimuthally symmetrical function of θ only, with θ being zero at the zenith (spherical coordinates). The solid angle element is $d\Omega = \sin \theta d\theta d\phi$. The beam solid angle is thus:

$$\Omega_A = \int_{2\pi} d\phi \int_0^\pi \sin \theta \exp(-\theta^2/2\sigma^2) d\theta$$

If we assume that

5.3 What do radio telescopes measure?

Convolution by the beam.

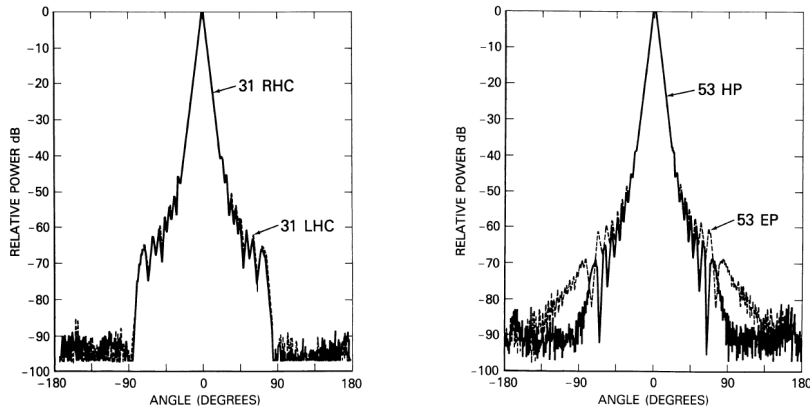


Figure 18: The measured beam pattern of the 31 GHz and 54 GHz channels of the DMR instrument on COBE. Each channel is sensitive to two polarizations (circular and linear for the 31 GHz and 54 GHz channels, respectively). Note the reduction of the minor lobes to below -50 dB (a factor of 10^5).

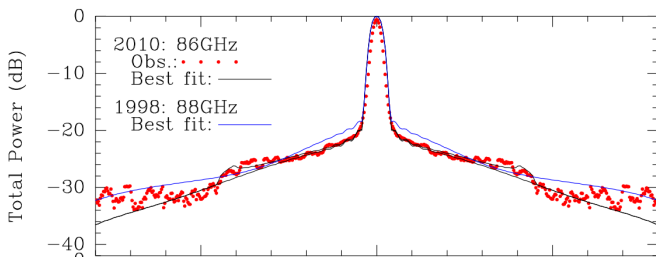


Figure 19: The measured beam pattern of the 3mm channel of EMIR at the IRAM-30m telescope (from Kramer & Greve 2013 IRAM Report. See also Greve et al 1998).

5.4 Observing modes

Because the atmosphere is a strong emitter at cm to sub-mm wavelengths, the scientific signal can only be recovered by means of a sky subtraction procedure. Sky brightness fluctuations dominate the noise. Different schemes are used depending on the type of observation, spectral lines or bolometric. The most basic switching mode is the so-called position-switching, where the primary is moved alternatively between an ON and an OFF positions, with the latter being free of extraterrestrial signal at the observation frequency. Subtraction of the two, ON-OFF, efficiently suppresses the offset due to atmospheric emission:

$$\text{Signal} = \text{ON} - \text{OFF}$$

However, depending on the time constant of the variations of the atmospheric water vapour content, different schemes may have to be used, such as a chopping secondary which can switch between the ON and OFF at a few Hz. For spectral line measurements, the frequency switching is another, powerful, method, which does not switch between an OFF and ON on the sky but in the frequency domain. This is achieved by changing the LO frequency a few MHz apart.

6 Temperature scales

The specific intensity unit in radio astronomy is very often the Kelvin, rather than SI units ($\text{W Hz}^{-1} \text{sr}^{-1} \text{m}^{-2}$) or Jansky (Jy). This is not only historical but also because it brings you directly to the right order of magnitude, while manipulating reasonable numbers. Simply speaking, this is very well adapted scale. Let us see why.

The main reason for using a temperature scale is that many radio sources are thermal sources (dust, CMB) hence, the temperature scale gives directly some insight into one physical property of the source. Also, the various contributions to the noise (atmosphere, ground, instrumental components) emit at black-bodies and their temperature therefore directly compares their contribution, which can also be compared to that of the astrophysical source.

Furthermore, radio astronomy was first developed at wavelengths where the Rayleigh-Jeans approximation, $h\nu \ll kT$, is a good one, such that the black-body radiation simplifies into a linear function of temperature:

$$B_\nu(T) = \frac{2hc^3}{\nu^2} \frac{1}{\exp h\nu/kT - 1} \approx \frac{2k\nu^2}{c^2} T$$

Therefore, many figures of merit of the instrument are expressing in a temperature scale, e.g. dark current of a receiver is not given in e-/s, but in K.

However, most of the temperatures that are quoted are not true temperatures, because thermal equilibrium is more the exception than the rule in the Universe (which includes the Earth, and us). Therefore, the temperatures are not always physical ones, but rather a number that has the dimension of it.

6.1 The antenna temperature

Probably the most fundamental temperature in radio astronomy is the so-called *antenna temperature*, noted T_A , which is *not* the physical temperature of, e.g. the primary mirror. Actually, this would be the case if the entire

telescope (mirrors, detectors, etc) was in thermal equilibrium with the incoming radiation from a black-body. This would require that there was nothing else at any other temperature, and that radiation and matter has exchanged for sufficient time such that all degrees of freedom have relaxed towards equilibrium at temperature T_A . This situation is quite excluded. Nevertheless, the concept of T_A remains powerful, as it indicates how much energy the telescope has measured.

6.2 The main-beam temperature

6.3 Noise and the radiometer formula

6.3.1 The receiver temperature

6.3.2 The system temperature

6.3.3 The radiometer formula

7 Bolometers

We note that bolometers sensitivity is not limited by quantum noise limit but are limited by **photon statistics**. Their resolving power is primarily set by filters, and have typically $R \sim 10$. The gap between $R \sim 10$ and 4000 is filled in by Fourier Transform Spectrometers (FTS) that are placed in the optical path towards a bolometer detector, such as the **SPIRE** facility onboard the Herschel satellite, which had $R_{\max} \sim 1000$ at wavelength between 250 and $500 \mu\text{m}$. The spectral resolution of FTS is limited mechanically by the length of the optical path L ($\delta\nu \approx c/4L$). In such a device, the spectral information is obtained by observing the source repetitively while varying L . Grating spectrometers (see Lecture on spectrometers) are alternative setups which allow similar resolving powers to be achieved. The PACS facility onboard Herschel is one example, reaching $R \sim 4000$.